PROCEEDINGS OF SCIENCE

Shell model calculations of nuclei around ^{208}Pb

E. Teruya*
Saitama University
E-mail: teruya@nuclei.th.phy.saitama-u.ac.jp

N. Yoshinaga
Saitama University
E-mail: yoshinaga@phy.saitama-u.ac.jp

K. Higashiyama
Chiba institute of technology
E-mail: koji.higashiyama@it-chiba.ac.jp

The large-scale shell-model calculation is performed for heavy nuclei which have more than 126 neutrons and 82 protons around the doubly magic nucleus ^{208}Pb. Seven single-particle orbitals above the magic number 126 and six single-particle orbitals between the magic numbers 82 and 126 are taken for neutrons and protons, respectively. As for a phenomenological interaction, one set of the interaction strengths, which consists of the multipole-paring interactions including the monopole pairing and quadrupole-quadrupole interactions is employed for all the nuclei considered. The energy spectra and electromagnetic properties are calculated and compared with the experimental data.

The 26th International Nuclear Physics Conference
11-16 September, 2016
Adelaide, Australia

*Speaker.

PoS(INPC2016)066

1. Introduction

Microscopic structure of nuclei around ^{208}Pb has not been studied enough. Theoretically, single-closed nuclei [1, 2, 3] and nuclei with a few valence nucleons [4, 5, 6] were studied using the shell model approach. However, open-shell nuclei which are far from the doubly magic nucleus ^{208}Pb have not been studied enough using the microscopic shell model due to its computational difficulties. In our group, we have developed the large-scale shell model code and carried out the systematic shell-model calculations for even-even, odd-mass, and doubly nuclei for nuclei which have less than 126 neutrons and more than 82 protons around ^{208}Pb [7]. Good agreements with experimental data were obtained not only for even-even nuclei, but also for odd-mass and doubly-odd nuclei. As a next challenge, we apply our shell-model code to nuclei which have more than 126 neutrons and 82 protons and perform a systematic analysis for these nuclei. Energy levels and electromagnetic properties are calculated and compared with the experimental data.

2. Theoretical framework

For single-particle levels, seven orbitals above the magic number 126, $1g_{9/2}$, $0i_{11/2}$, $0j_{15/2}$, $2d_{5/2}$, $3s_{1/2}$, $2g_{7/2}$, and $2d_{3/2}$ are taken for neutrons. For protons, all the six $0h_{9/2}$, $1f_{7/2}$, $0i_{13/2}$, $2p_{3/2}$, $1f_{5/2}$, and $2p_{1/2}$ orbitals in the major shell between the magic numbers 82 and 126 are taken. Both neutrons and protons are treated as particles. The single-particle energies ε_τ ($\tau = \nu$ or π) employed in the present calculations are listed in Table 1. Single-particle energies of neutrons (protons) are adapted from the experimental energy levels of ^{209}Pb (^{209}Bi). Here, particle number dependences on single-particle energies are assumed for the neutron $0j_{15/2}$ orbital and the proton $0i_{13/2}$ and $1f_{7/2}$ orbitals as follows in unit of MeV:

$$\varepsilon_\nu(0j_{15/2}) = 0.20N_\nu - 0.150N_\pi + 1.223, \tag{2.1}$$
$$\varepsilon_\pi(0i_{13/2}) = -0.050N_\pi + 1.659, \tag{2.2}$$
$$\varepsilon_\pi(1f_{7/2}) = 0.031N_\nu + 0.869, \tag{2.3}$$

where N_ν and N_π represent the numbers of valence neutron and valence proton particles, respectively. These number dependences conform with the experimentally suggested value in ^{209}Pb and ^{209}Bi. These particle number dependences are introduced for a better reproduction of low-lying states.

A phenomenological interaction is used in this study. The Hamiltonian consists of the pairing plus quadrupole-quadrupole and multipole interaction, which is the same as described in Ref. [7]. The adopted strengths of two-body interactions are listed in Table 2. Only one set of strengths is adopted for all the nuclei discussed in this paper.

For $E2$ transition rates and quadrupole moments, the effective charges are taken as $e_\nu = 1.0e$ for neutrons and $e_\pi = 1.50e$ for protons. For magnetic moments, the adopted gyromagnetic ratios for orbital angular momenta are $g_{\ell\nu} = 0.00$, $g_{\ell\pi} = 1.00$, and those for spin are $g_{s\nu} = -2.87$ and $g_{s\pi} = 2.79$. These effective charges and gyromagnetic ratios are adjusted to reproduce the experimental data in single-closed nuclei. Further details of the shell-model framework and electromagnetic transition operators are presented in Refs. [7, 8].

Table 1: Adopted single-particle energies ε_τ ($\tau = \nu$ or π) for neutrons and protons (in unit of MeV). The energies for the neutron $0j_{15/2}$ orbital and the proton $0i_{13/2}$ and $1f_{7/2}$orbitals are changed linearly with numbers of valence neutron (N_ν) and proton particles (N_π). Definitions of the $\varepsilon_\nu(0j_{15/2})$, $\varepsilon_\pi(i_{13/2})$, and $\varepsilon_\pi(f_{7/2})$ are given in Eqs. (2.1), (2.2), and (2.3).

j	$1g_{9/2}$	$0i_{11/2}$	$0j_{15/2}$	$2d_{5/2}$	$3s_{1/2}$	$2g_{7/2}$	$2d_{3/2}$
ε_ν	0.000	0.779	$\varepsilon_\nu(j_{15/2})$	1.567	2.032	2.491	2.538
j	$2p_{1/2}$	$1f_{5/2}$	$2p_{3/2}$	$0i_{13/2}$	$1f_{7/2}$	$0h_{9/2}$	
ε_π	3.634	2.826	3.119	$\varepsilon_\pi(i_{13/2})$	$\varepsilon_\pi(f_{7/2})$	0.000	

Table 2: Strengths of adopted two-body interactions between neutrons (ν-ν) and those between protons (π-π). G_0 and G_2 indicate the strengths of the monopole (*MP*) and quadrupole-pairing (*QP*) interactions between like nucleons. G_L ($L = 4, 6, 8, 10$) denote the strengths for higher multipole-pairing (*HMP*) interactions between like nucleons. The strength of the proton two-body interaction between the $0h_{9/2}$ and $1f_{7/2}$ orbitals (*MP*-8) is taken as $G^{(8)}_{\pi h_{9/2} f_{7/2}} = 0.50$. The strength of the $Q_\nu Q_\pi$ interaction between neutrons and protons is taken as $\kappa_{\nu\pi} = 0.080$. The strengths of the *MP*, *HMP*, and *MP*-8 interactions are given in units of MeV. The strengths of the *QP* and *QQ* interactions are given in units of MeV$/b^4$ using the oscillator parameter b.

	G_0	G_2	G_4	G_6	G_8	G_{10}
ν-ν	0.102	0.008	0.400	0.300	0.000	0.450
π-π	0.145	0.013	0.400	0.400	−0.600	0.000

3. Theoretical results

The theoretical results are given for each nucleus. The energy spectra, $E2$ transition rates, magnetic moments, and quadrupole moments are calculated. For energy spectra, up to four observed energy levels are shown from the yrast state for each spin and parity in experiment. As for the theoretical states, two levels from the lowest level for each spin and parity are shown in general. If third or fourth states are observed in experiment, third or fourth energy levels are shown in theory.

3.1 Pb isotopes

Here ^{210}Pb and ^{212}Pb are discussed. Figure 1 shows the theoretical energy spectra for ^{210}Pb and ^{212}Pb in comparison with the experimental data [9, 10, 11]. ^{210}Pb is a system with two neutron particles outside the doubly magic core ^{208}Pb. This nucleus tells us information about the interaction between two neutrons. The calculation reproduces energy levels of yrast 0^+_1, 2^+_1, $\cdots$, 10^+_1 states well. The narrow energy gaps between the 6^+_1 and 8^+_1 states and the 4^+_1 and 6^+_1 states are well reproduced. The 6^+_1 and 8^+_1 states are isomers with half lives of 49 ns and 201 ns, respectively [9].

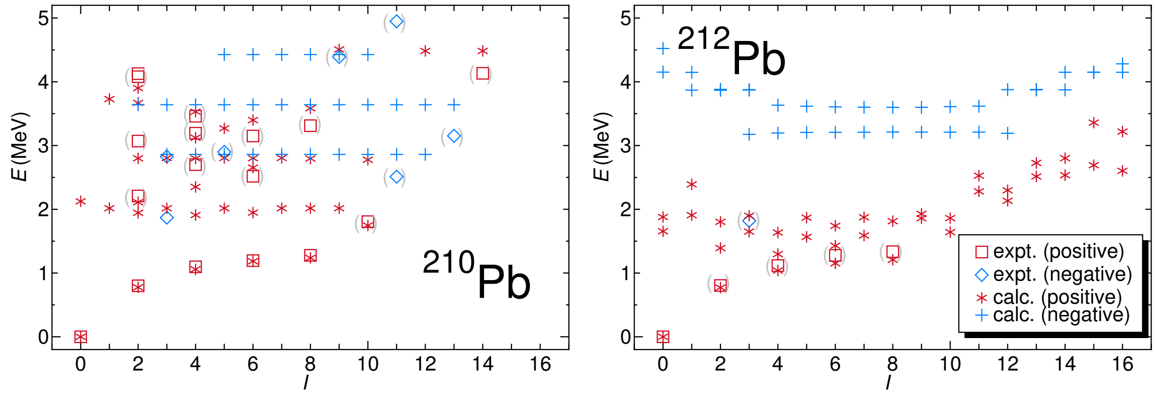

Figure 1: Theoretical energy spectra for ^{210}Pb and ^{212}Pb in comparison with the experimental data. The squares and diamonds represent experimental positive and negative parity states, respectively. The asterisks and crosses represent theoretical positive and negative parity states, respectively. The experimental data are taken from Refs. [9, 10, 11]. Ambiguous states are shown with parentheses.

Table 3: Comparison between the experimental $B(E2)$ values (expt.) and the theoretical results (calc.) for ^{210}Pb and ^{212}Pb (in W.u.). The experimental data are taken from Refs. [9, 10].

^{210}Pb	expt.	calc.
$2_1^+ \to 0_1^+$	1.4(4)	3.113
$4_1^+ \to 2_1^+$	4.8(9)	3.307
$6_1^+ \to 4_1^+$	2.1(8)	2.109
$8_1^+ \to 6_1^+$	0.7(3)	0.759
$10_1^+ \to 8_1^+$		0.018
^{212}Pb	expt.	calc.
$2_1^+ \to 0_1^+$		4.961
$4_1^+ \to 2_1^+$		0.565
$6_1^+ \to 4_1^+$		0.339
$8_1^+ \to 6_1^+$		0.119
$10_1^+ \to 8_1^+$		0.082

The experimentally unobserved 12_1^+ state is calculated at 4.484 MeV. The almost degenerate 3_1^-, 4_1^-, $\cdots$, 12_1^- states at around 2.9 MeV consist of the $(\nu g_{9/2} j_{15/2})$ configuration. The almost degenerate 2_1^-, 3_2^-, $\cdots$, 13_1^- states at around 3.7 MeV consist of the $(\nu i_{11/2} j_{15/2})$ configuration. Similarly, the almost degenerate 5_3^-, 6_3^-, $\cdots$, 10_3^- states at around 5.5 MeV consist of the $(\nu j_{15/2} d_{5/2})$ configuration. In ^{212}Pb, spin is assigned for only several positive parity states in experiment. The yrast band is well reproduced in the calculation. The experimentally unobserved 10_1^+ state is calculated at 1.642 MeV. The experimental 3_1^- states are located at 1.870 MeV and 1.820 MeV for ^{210}Pb and ^{212}Pb, respectively. These states are made by core excitations [12] and out of the present framework. The low-lying 3^- states which are made by core excitations are seen in Pb isotopes in the

Table 4: Comparison of the magnetic dipole moments μ (in μ_N) and the electric quadrupole moments Q (in eb) obtained by the shell model (calc.) to the experimental data (expt.) for Pb isotopes. The experimental data are taken from Refs. [9, 10].

	μ		Q	
^{210}Pb	expt.	calc.	expt.	calc.
2_1^+		-0.360		+0.021
4_1^+		-1.026		+0.035
6_1^+	$-1.872(90)$	-1.811		-0.104
8_1^+	$-2.496(64)$	-2.551		-0.436
10_1^+		-0.208		-0.678
^{212}Pb	expt.	calc.	expt.	calc.
2_1^+		-0.425		+0.068
4_1^+		-1.067		+0.071
6_1^+		-1.785		+0.066
8_1^+		-2.469		+0.130
10_1^+		-0.211		+0.505

mass region 210 as discussed in Ref. [7].

Calculated results of the $B(E2)$ values, magnetic moments, and quadrupole moments for ^{210}Pb and ^{212}Pb are given in Tables 3 and 4 in comparison with the experimental data [9, 10]. Most of experimental values are well reproduced in the calculation. The largest discrepancy between the experimental value and the theoretical one is seen in the $B(E2; 2_1^+ \to 0_1^+)$ value of ^{210}Pb. The calculated result is 2.2 times larger than the experimental one. The $B(E2; 10_1^+ \to 8_1^+)$ values of ^{210}Pb and ^{212}Pb are calculated much smaller than other transition rates among yrast states. The 0_1^+, 2_1^+, $\cdots$, 8_1^+ states consist of neutrons in the $1g_{9/2}$ orbitals. However, one neutron needs to be excited to the $0i_{11/2}$ orbital to make the 10_1^+ state and the configuration is changed from the 8_1^+ state to the 10_1^+ state.

3.2 Po isotopes

Here ^{212}Po and ^{214}Po are discussed. Figure 2 shows the theoretical energy spectra for ^{212}Po and ^{214}Po in comparison with the experimental data [9, 11, 13]. ^{212}Po is a system with two valence neutrons and two valence protons. The narrow energy gap between the 6_1^+ and 8_1^+ states is well reproduced. The 0_1^+, 2_1^+, $\cdots$, 8_1^+ states mainly consist of the $(\nu g_{9/2}^2 \pi(h_{9/2})^2_{0^+})$ configuration. In contrast, the 10_1^+ state consists of the $(\nu g_{9/2} h_{11/2} \pi(h_{9/2})^2_{0^+})$ configuration and the 12_1^+ and 14_1^+ states consist of the $(\nu g_{9/2}^2 \pi h_{9/2}^2)$ configuration. The negative parity states which are calculated at around 2.5 MeV are members of the $(\nu h_{9/2}^2 \pi g_{9/2} i_{13/2})$ configuration. In ^{214}Po, only the 0_1^+, 2_1^+, and 4_1^+ states are observed in yrast states. The 6_1^+, 8_1^+, and 10_1^+ states are calculated at 1.395, 1.505, and 1.806 MeV, respectively. The state at 1.275 MeV is assigned as (3^-) [16]. The theoretical first 3^- state is calculated at 3.036 MeV. The experimental (3_1^-) state is supposed to be an octupole state [16]. In this mass region, the importance of the octupole correlation is known. The state at

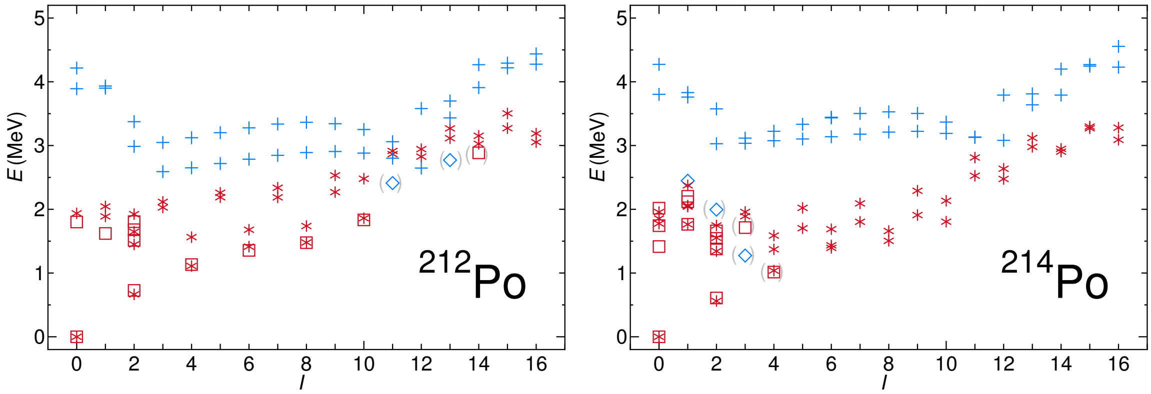

Figure 2: Same as fig. 1, but for ^{212}Po and ^{214}Po. The experimental data are taken from Refs. [9, 11, 13].

Table 5: Same as table 3, but for ^{212}Po and ^{214}Po. The experimental data are taken from Refs. [9, 11, 13].

^{212}Po	expt.	calc.
$2_1^+ \to 0_1^+$		10.806
$4_1^+ \to 2_1^+$		12.966
$6_1^+ \to 4_1^+$	3.9(11)	9.689
$8_1^+ \to 6_1^+$	2.30(9)	3.895
$10_1^+ \to 8_1^+$	2.2(6)	0.138
^{214}Po	expt.	calc.
$2_1^+ \to 0_1^+$		17.583
$4_1^+ \to 2_1^+$		23.208
$6_1^+ \to 4_1^+$		18.290
$8_1^+ \to 6_1^+$		7.825
$10_1^+ \to 8_1^+$		0.560
$0_2^+ \to 2_1^+$	0.159(10)	0.714

1.995 MeV which is assigned as (2_1^-) state is also considered to be the coupling state of the octupole state and the quadrupole phonon state. In our calculation, negative parity states are calculated above 3.0 MeV.

The calculated $B(E2)$ values, magnetic moments, and quadrupole moments for Po isotopes are given in Tables 5 and 6 in comparison with the experimental data [9, 11, 13, 15]. In ^{212}Po, the calculated $B(E2;10_1^+ \to 8_1^+)$ value is much smaller than the experimental value.

3.3 Rn isotopes

Here ^{214}Rn and ^{216}Rn are discussed. Figure 3 shows the theoretical energy spectra for ^{214}Rn and ^{216}Rn in comparison with the experimental data [9, 13, 14]. Yrast states are well reproduced for both nuclei. The spin and parity of the state at 1.332 MeV of ^{214}Rn are not assigned. This state decays to the 2_1^+ state at 0.695 MeV. In our calculation, the 2_2^+ state is calculated at 1.563 MeV.

Table 6: Same as table 4, but for ^{212}Po and ^{214}Po.

	μ		Q	
^{212}Po	expt.	calc.	expt.	calc.
2_1^+		+0.246		+0.049
4_1^+		−0.096		+0.057
6_1^+		−1.092		−0.065
8_1^+		−2.299		−0.104
10_1^+		−0.080		−0.191
^{204}Po	expt.	calc.	expt.	calc.
2_1^+		+0.273		+0.110
4_1^+		+0.268		+0.180
6_1^+		−0.513		+0.232
8_1^+		−1.939		+0.088
10_1^+		−0.059		+0.247

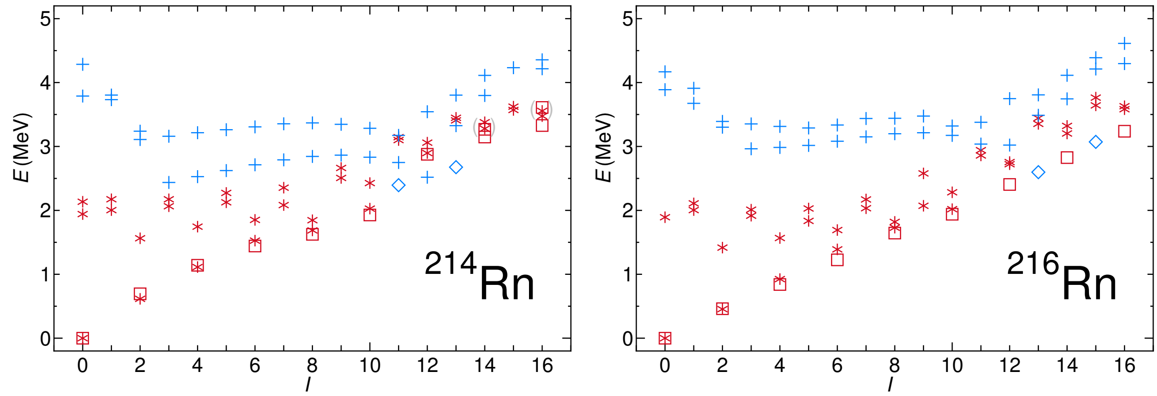

Figure 3: Same as fig. 1, but for ^{214}Rn and ^{216}Rn. The experimental data are taken from Refs. [9, 13, 14].

From our calculation and comparison with neighboring nuclei, it is suggested that the spin and parity of the state at 1.332 MeV is 2^+. The spin and parity of the state at 1.838 MeV is assigned as $(8^+, 9^+, 10^+)$. The 8_2^+, 9_1^+, and 10_2^+ states are calculated at 1.820, 2.072, and 2.283 MeV. Thus our calculation suggests that the spin and parity of the state at 1.838 MeV is 8^+. A specific feature of even-even nuclei in this region is the narrow energy gap between the 6_1^+ and 8_1^+ state. In ^{216}Rn, however, the narrow energy gap between the 6_1^+ and 8_1^+ state is not seen in experiment anymore and the calculation reproduces this feature.

Calculated results of the $B(E2)$ values, magnetic moments, and quadrupole moments for Rn isotopes are given in Tables 7 and 8 in comparison with the experimental data [9, 13]. The calculation predicts large $B(E2)$ values between yrast states in even-even Rn isotopes, However, the observed $B(E2; 6_1^+ \to 4_1^+)$ and $B(E2; 8_1^+ \to 6_1^+)$ values are much smaller.

Table 7: Same as table 3, but for ^{214}Rn and ^{216}Rn. The experimental data are taken from Refs. [9, 13].

^{214}Rn	expt.	calc.
$2_1^+ \to 0_1^+$	>0.032	18.023
$4_1^+ \to 2_1^+$	>0.28	23.924
$6_1^+ \to 4_1^+$	3.8^{+17}_{-9}	20.273
$8_1^+ \to 6_1^+$	3.3^{+3}_{-1}	10.148
$10_1^+ \to 8_1^+$	2.9(7)	0.602
$12_1^+ \to 10_1^+$	>0.0064	0.008
$14_1^+ \to 12_1^+$		18.93
$16_1^+ \to 14_1^+$	≤4.4(3)	7.412
$18_1^+ \to 16_1^+$	0.71(5)	0.530
$13_1^- \to 11_1^-$	0.93(8)	0.126
^{216}Rn	expt.	calc.
$2_1^+ \to 0_1^+$		27.982
$4_1^+ \to 2_1^+$		39.596
$6_1^+ \to 4_1^+$		38.507
$8_1^+ \to 6_1^+$		20.939
$10_1^+ \to 8_1^+$		2.137

Table 8: Same as table 4, but for ^{214}Rn and ^{216}Rn.

	μ		Q	
^{214}Rn	expt.	calc.	expt.	calc.
2_1^+		+0.421		+0.002
4_1^+		+0.294		+0.040
6_1^+		−0.684		−0.020
8_1^+		−2.018		−0.193
10_1^+		+0.021		−0.881
^{216}Rn	expt.	calc.	expt.	calc.
2_1^+		+0.443		−0.003
4_1^+		+0.616		+0.005
6_1^+		+0.256		+0.010
8_1^+		−1.295		−0.025
10_1^+		+0.089		+0.011

4. Summary

In this study, the large-scale shell-model calculation has been performed for nuclei which have more than 126 neutrons and more than 82 protons around ^{208}Pb using one set of the phenomenological interactions. The energy spectra, $E2$ transition rates, magnetic moments and quadrupole moments have been calculated and compared with the experimental data. Good agreements with the experimental data have been obtained.

Acknowledgment

This work was supported by Grant-in-Aid for Scientific Research (C) (No. 16K05341) and (No. 25400267) from Japan Society for the Promotion of Science (JSPS), and also by Grant-in-Aid for JSPS Fellows Grant Number 2610429.

References

[1] J. B. Mcgrory, and T. T. S. Kuo, Nucl. Phys. A **247**, 283 (1975).

[2] L. Coraggio, A. Covello, A. Gargano, N. Itaco, and T. T. S. Kuo, Phys. Rev. C **60**, 064306 (1999).

[3] E. Caurier, M. Rejmund, and H. Grawe, Phys. Rev. C **67**, 054310 (2003).

[4] C. W. Ma, and W. W. True, Phys. Rev. C **8**, 2313 (1973).

[5] P. Alexa, and R. K. Sheline, Phys. Rev. C **56**, 3087 (1997).

[6] L. Coraggio, A. Covello, and A. Gargano, and N. Itaco, Phys. Rev. C **76**, 061303 (2007).

[7] E. Teruya, K. Higashiyama, and N. Yoshinaga, Phys. Rev. C **93**, 064327 (2016).

[8] E. Teruya, N. Yoshinaga, K. Higashiyama, and A. Odahara, Phys. Rev. C **92**, 034320 (2015).

[9] Evaluated Nuclear Structure Data File (ENSDF),[http://www.nndc.bnl.gov/ensdf/] .

[10] M. S. Basunia, Nucl. Data Sheets. **121**, 561 (2014).

[11] E. Browne, Nucl. Data Sheets. **104**, 427 (2005).

[12] E.R. Flynn, G.J. Igo, R.A. Broglia, S. Landowne, V. Paar, and B. Nilsson, Nucl. Phys. A **195**, 97 (1972).

[13] S.-C. Wu, Nucl. Data Sheets. **110**, 681 (2009).

[14] S.-C. Wu, Nucl. Data Sheets. **108**, 1057 (2007).

[15] M. D. Seliverstov, *et al.*, Phys. Rev. C **89**, 034323 (2014).

[16] H. W. Taylor, B. Singh, and D. A. Viggars, Phys. Rev. C **34**, 2322 (1986).